

Tfet Biosensor Simulation and Analysis for Various Biomolecules

P Vimala (✉ ervimala@gmail.com)

Dayananda Sagar College of Engineering <https://orcid.org/0000-0002-8247-6621>

Likith Krishna L

Dayananda Sagar College of Engineering

Sharma SS

Dayananda Sagar College of Engineering

Rakshanda Ainapur

Dayananda Sagar College of Engineering

Swetha RH

Dayananda Sagar College of Engineering

Research Article

Keywords: TFET, nanocavity, Drain current, Gate Voltage, Biomolecules, Bio sensing, ON current

Posted Date: September 14th, 2021

DOI: <https://doi.org/10.21203/rs.3.rs-870076/v1>

License:   This work is licensed under a Creative Commons Attribution 4.0 International License.

[Read Full License](#)

Version of Record: A version of this preprint was published at Silicon on January 19th, 2022. See the published version at <https://doi.org/10.1007/s12633-021-01570-x>.

Abstract

This paper investigates the simulation and performance of Tunnel field effect transistor (TFET) with a nanocavity in it, which can be used for bio sensing application. The entire simulation is done using the tool Silvaco Atlas TCAD. This paper mainly aims in comparing the different parameters for few biomolecules which has different dielectric constant values, namely Streptavidin, Biotin, APTES, Cellulose and DNA. The device structure here consists of a nanocavity near the source end, which is used to place these biomolecules and hence observe the variation of the Drain current v/s Gate voltage characteristic graph, these biomolecules that are having unique dielectric constants are placed within this cavity and these graphs are observed. The energy band diagram of this device is obtained; on top of this various other parameters namely Surface Potential, Electric field are observed for the above-mentioned Biomolecules. The Length of the cavity of the biosensor is also varied to observe the difference, in addition to this Ion (ON current) variation is plotted for the change in the dielectric constant of the biomolecule.

1 Introduction

Biological monitoring and the processes involving biochemical substances are important for biological and medical applications. Biosensors that are highly sensitive, cost-effective, and very specific are in demand since they put up to the realization of extremely accurate diagnosis of certain medicines. Hence, various biosensors have been studied extensively because of inception of first-generation biosensors that utilized glucose oxidase during 1962 [1].

A Biosensor is an analytical device that produces electrical signals by detecting changes in biological processes. A biological process is a term which can be any of the following biological element or material like enzymes, tissues, microorganisms or cells. Biosensors that are based on FETs are in popular use because of their excellence in label-free electrical detection, ultra-sensitivity, very less production cost and, mass manufacturing ability. The flow of current is controlled by electric field in FETs [2,3]. FET based biosensors are used to detect biological species owing to miniaturization, cost-effectiveness, and label-free detection [4]. Biosensors that were based on FETs were utilized as Ion Sensitive Field Effect Transistor (ISFET) in the beginning. The diagnosis of neutral biomolecules that was difficult for ISFET was succeeded by using Impact Ionization Junction less FET (JFET) along with MOSFET (IMOS) which became the other novel device technologies reported for biosensing applications [5–7]. These devices suffered from various issues like very high off-state leakage current, low drive current, random dopant fluctuations which was highly complex when it came to fabrication. In IMOS, current was injected in the presence of a high intensity of electric field in to drain end. This process requires a higher drain to source bias voltage. In addition to this, the manufacturing of this device is extremely complex which is under sub-40 nm gate length [8–10]. Consequently, Impact Ionisation MOSFET was disregarded for low-power and ultra-sensitive biosensors. Junction FET suffered adversely because it is based on reverse-biased semiconductor junction and therefore has some gate leakage current due to the presence of minority

charge carriers [11–13]. This resulted in static power dissipation and low- sensitivity of JFET and affected its application in biosensors [14,15].

This paper focuses on finding the impact of introducing materials with different dielectrics namely Steptavidin, Biotin, Aminopropyltriethoxysilane (APTES), Cellulose, and Deoxyribonucleic acid (DNA), and observing its I-V characteristics. From carefully analyzing the simulation results, we can infer that TFET is suitable for biosensing applications. The device simulation is carried out in Silvaco ATLAS TCAD, and the graphs are also plotted with the same tool, along with this MATLAB from Math Works is used to plot few graphs.

2 Device Structure

Figure 1 shows the structure of the proposed device which is Tunnel field Effect Transistor (TFET) with a Nano cavity used for biosensing application. It consists of four main regions namely Source, Drain, and Channel which is yellow, and oxide region that is indicated by blue color. Along with this, it consists of two gate electrodes, a source, and a drain electrode each of which is indicated by a thin blue line that can be observed in the figure. The major difference observed here in this structure when compared to the TFET structure is the nanocavity region which is indicated by the red color. Here nanocavity plays an important role in which the molecules with different dielectrics are placed. The source and drain are 25 nm each, and the length of nanocavity is 25 nm, the overall channel length is 50nm. Table.1 listed the parameters and its value used for simulation.

Table 1. Parameters, Symbols and Its values used in Simulation

Sl. No	Parameter	Symbol	Values
1.	Length of Source	L_s	25nm
2.	Length of cavity	L_c	25nm
3.	Length of Drain	L_D	0.75nm
4.	Length of Gate	L_G	50nm
5.	Work Function of Gate Material	ϕ_G	4.2eV
6.	Work Function of Source and Drain	ϕ_S, ϕ_D	4.2eV
7.	Doping Concentration of Source (N-type)	N_S	$1 \times 10^{20}/\text{cm}^3$
8.	Doping Concentration of Drain (N-type)	N_D	$1 \times 10^{16}/\text{cm}^3$
9.	Doping Concentration of Channel (N-type)	N_{CH}	$5 \times 10^{18}/\text{cm}^3$

3 Results And Discussion

Figure 2 indicates energy band diagram with respect to various biomolecules of Biosensor of this proposed device structure for biomolecules having various dielectric constants shown in table.2. Electrons need the energy to jump from a lower energy level to a higher energy level. The dotted lines in the graph indicate the valence band and solid lines indicate the conduction band. The bandgap before tunneling is approximately 1eV. During tunneling, different energy levels in valence and conduction band can be observed for different biomolecules.

Table 2
Biomolecules with their Dielectric Values

Sl. No	Biomolecules	Dielectric Constant
1	DNA	8.7
2	Cellulose	6.1
3	Biotin	2.63
4	Streptavidin	2.1
5	APTES	3.57

Fig. 3 indicates variation of Potential for various dielectric values. Potential is minimum at the Source region and starts increasing across the channel and further increases in the Drain region. The potential starts from -0.64V and saturates at 1.51V. For different values of dielectric constant, the potential of the

device changes. From the graph, we can observe that the steep and high potential is obtained for a greater value of the dielectric constant. **Fig.4** indicates variation of Electric Field across channel of this device. In the graph, we can observe two peaks since we have two gates for our device structure. At each point, the electric field is measured, and the sharp points denote the junction. For DNA having the dielectric constant $K=8.7$, the electric field is 2.28×10^6 and 1.0×10^5 . For Cellulose having dielectric constant $K=6.1$, the electric field is 2.16×10^6 and 1.0×10^5 . For APTES having the dielectric constant $K=3.57$, the electric field is 1.97×10^6 and 1.0×10^5 . For Biotin having the dielectric constant $K=2.63$, the electric field is 1.87×10^6 and 1.0×10^5 . For Streptavidin having the dielectric constant $K=2.1$, the electric field is 1.8×10^6 and 1.0×10^5 . For different values of dielectric constant, the electric field across the device changes. The electric field is directly proportional to the dielectric value and from the graph, we can observe that as we increase the value of dielectric constant the electric field across the device increases.

Figure 5 indicates plot of I-V Characteristics for different values of dielectric constants by plotting the drain current (I_D) in Amperes on the Y-axis, Gate voltage (V_G) in Volts on the X-axis. This voltage is varied in the steps of 0.05V. The channel length is kept constant at 50nm. From the figure, we observe that drain current increases as gate voltage increases from 0.1V to 1V. For Streptavidin having the dielectric constant, $K = 2.1$ the value of I_D starts increasing from 0.9V. For biotin having the dielectric constant $K = 2.63$ the value of I_D starts increasing from 0.75V. For APTES having the dielectric constant of $K = 3.57$ the value of I_D starts increasing from 0.55V and saturates at drain current 4×10^{-8} A and 1V. For Cellulose having a dielectric constant of $K = 6.1$ the value of I_D starts increasing from 0.3V and saturates at drain current 4×10^{-8} A and 1v. For DNA having the dielectric constant of $K = 8.7$ the value of I_D starts increasing from 0.15V and saturates at drain current 4×10^{-8} A and 1V.

Figure 6 indicates the plot of I-V Characteristics for different values of dielectric constants by plotting the drain current (I_D) in Amperes on the Y-axis, gate voltage (V_g) in Volts on the X-axis. The voltage is varied in the steps of 0.05V. The channel length is kept constant at 50nm. The Y-axis is in the logarithmic scale. For Dielectric constant $K = 2.1$ I_D is in the range of 10^{-12} A and saturates at the range of 10^{-7} A, similar characteristics are observed for all the materials with different dielectric values. All of these drain current values saturate at the range of 10^{-7} A as shown in the figure.

Figure 7 indicates the plot of I-V Characteristics for different values of cavity lengths by plotting the drain current (I_D) in Amperes on the Y-axis, gate voltage (V_g) in Volts on the X-axis. The cavity length is increased in the steps of 5nm. We have taken APTES Biomolecule of dielectric constant $K = 3.5$, which is a medium range of dielectric value. From the graph, we can observe that the value of I_D starts increasing from 0.55V and saturates at drain current 4×10^{-8} A and 1V.

Fig. 8 shows the influence of I_{ON} current on this proposed device structure for distinct values of various dielectric constants. Inferring the above figure, we discover the raise in dielectric constant considerably

raises the ON current. This is because an increase in k causes the electric current at the tunnel junction to increase, resulting in a reduction in tunnel width.

4 Conclusion

The study and analysis of the biosensor in this paper are done successfully using TFET with nanocavity. Energy band diagram of this device is obtained. Biomolecules consisting of unique dielectrics are placed within the cavity and the difference in I-V graphs are observed which leads us to a conclusion that the dielectric of the material placed has a major impact on I-V characteristics that can be utilized as a biosensor which detects the material that is placed inside the biosensor. The Electric field and Surface Potential characteristics of this biosensor for different biomolecules of varying dielectrics are compared. In addition to this, other conclusions such as I-V characteristic curve (Drain current v/s Gate voltage) is independent of cavity length of this proposed biosensor and on current (I_{on}) is increased with the increase in dielectric value of the biomolecule is also concluded.

Declarations

Funding: There is no financial support for this work.

Conflicts of interest/Competing interests: There is no conflict of interest

Availability of data and material: Not used any available data.

Code availability: Not used any available code

Ethics approval: Not applicable

Consent to participate: Not applicable

Consent for publication: Not applicable

Authors' contributions: Not applicable

Acknowledgements: Not applicable

References

1. Deblina Sarkar KB, Gossner H, Hansch W, Impact-ionization field-effect-transistor based biosensors for ultra-sensitive detection of biomolecules, *Appl. Phys. Lett.* 102 (2013)
2. Ebara M, Andrew W, *Biomaterials Nanoarchitectonics*, Tokyo, 2016
3. S.L. and Zhao SMQT, Rije E, Breuer U, Tuning of silicide Schottky barrier heights by segregation of sulfur atoms, in: *7th Int. Conf. Solid-State Integr. Circuits Technol.*, 2004: pp. 456–459

4. Sumit Kale PN, Kondekar (2016) Ferroelectric Schottky barrier tunnel FET with gate-drain underlap: Proposal and investigation. *Superlattices Microstruct* 89:225–230
5. Singh D, Pandey S, Nigam K, Sharma D, Yadav DS, Kondekar P (2017) A Charge-Plasma-Based Dielectric-Modulated Junctionless TFET for Biosensor Label-Free Detection. *IEEE Trans Electron Devices* 64:271–278
6. Buvaneswari B, Balamurugan NB (2019) 2D analytical modeling and simulation of dual material DG MOSFET for biosensing application. *AEU - Int J Electron Commun* 99:193–200
7. Im CY, Huang H, Gu XJ (2007) B, A dielectric-modulated field-effect transistor for biosensing. *Nat Nanotechnol* 2:430–434
8. Latha S (2020) N.K.H., Kale, Dielectric Modulated Schottky Barrier TFET for the Application as Label-Free Biosensor. *Silicon* 12:2673–2679
9. H.P. and Kim YCC, Jung C (2009) Novel dielectricmodulated field-effect transistor for label-free DNA detection. *Biochip J* 2:127–134
10. Lee C-W, Ferain I, Afzalain A (2010) Ran Yan, Nima Dehdashti Akhavan, Pedram Razavi, Jean-Pierre Colinge, Performance estimation of junctionless multigate transistors. *Solid State Electron* 54:97–103
11. Vimala P, Nithin Kumar NR (2019) Comparative Analysis of Various Parameters of Tri-Gate MOSFET with High-K Spacer. *JNanoR* 56:119–130
12. Kumar MJ, Janardhanan S (2013) Doping-Less Tunnel Field Effect Transistor: Design and Investigation. *IEEE Trans Electron Devices* 60:3285–3290
13. R.S.G. and Narang MGR, Reddy KVS, Saxena M (2015) A Dielectric-Modulated Tunnel-FET-Based Biosensor for Label-Free Detection: Analytical Modeling Study and Sensitivity Analysis. *IEEE Trans Electron Devices* 59:2809–2817
14. Usha C, Vimala P (2019) An Electrostatic Analytical Modeling of High-K stacked Gate-All-Around Heterojunction Tunnel FETs Considering the Depletion Regions, *AEU – Int. Jour of Elec Comm* 110:152877
15. V.N. and Jhaveri JCSWR (2009) Asymmetric Schottky Tunneling Source SOI MOSFET Design for Mixed-Mode Applications. *IEEE Trans Electron Devices* 56:93–99

Figures

ATLAS
Data from MAS_0%DLTFET.str

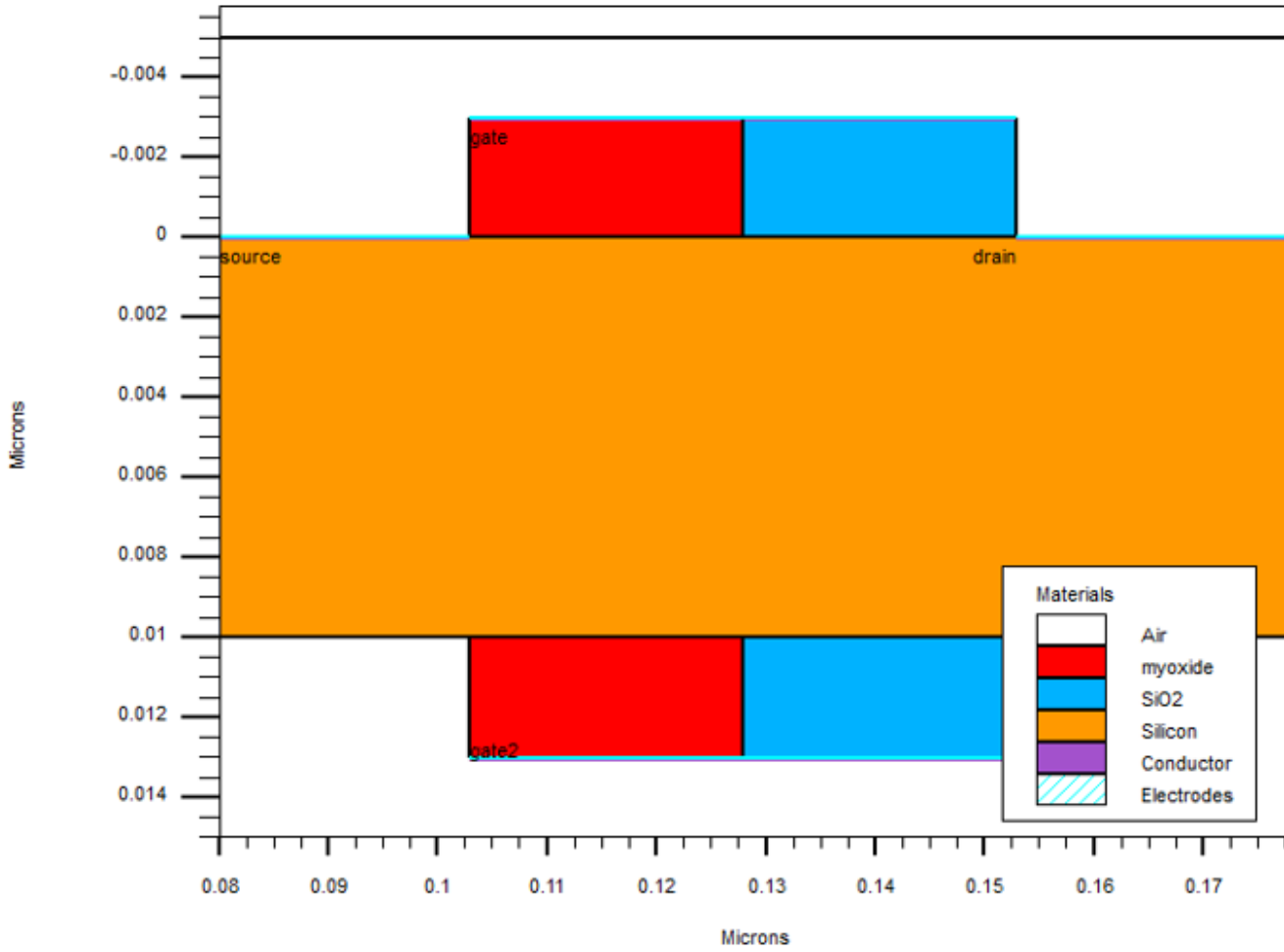


Figure 1

TFET Structure with Nanocavity

Conduction and Valance Band Energy Diagram

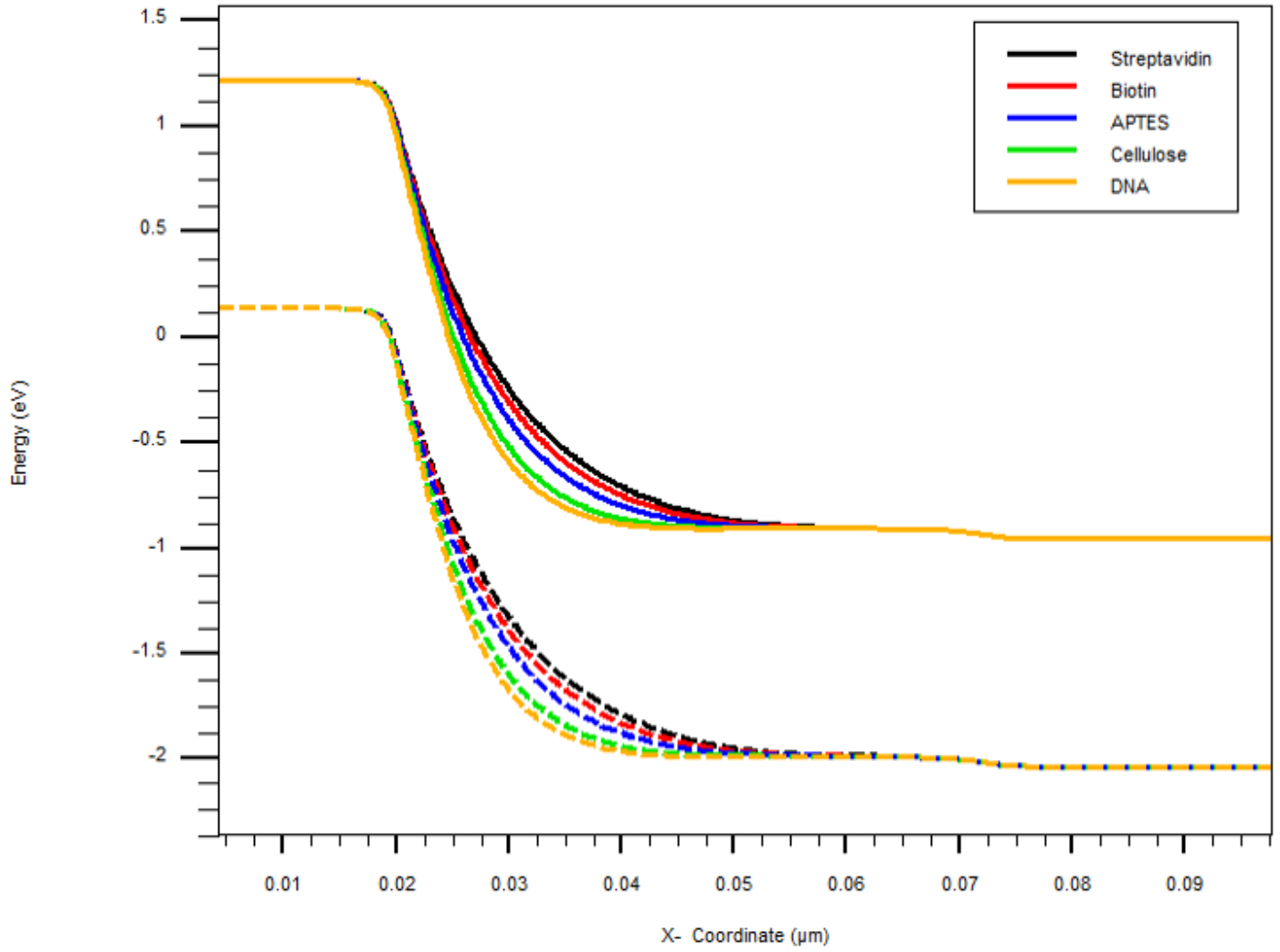


Figure 2

Energy band diagram with respect to various biomolecules of Biosensor

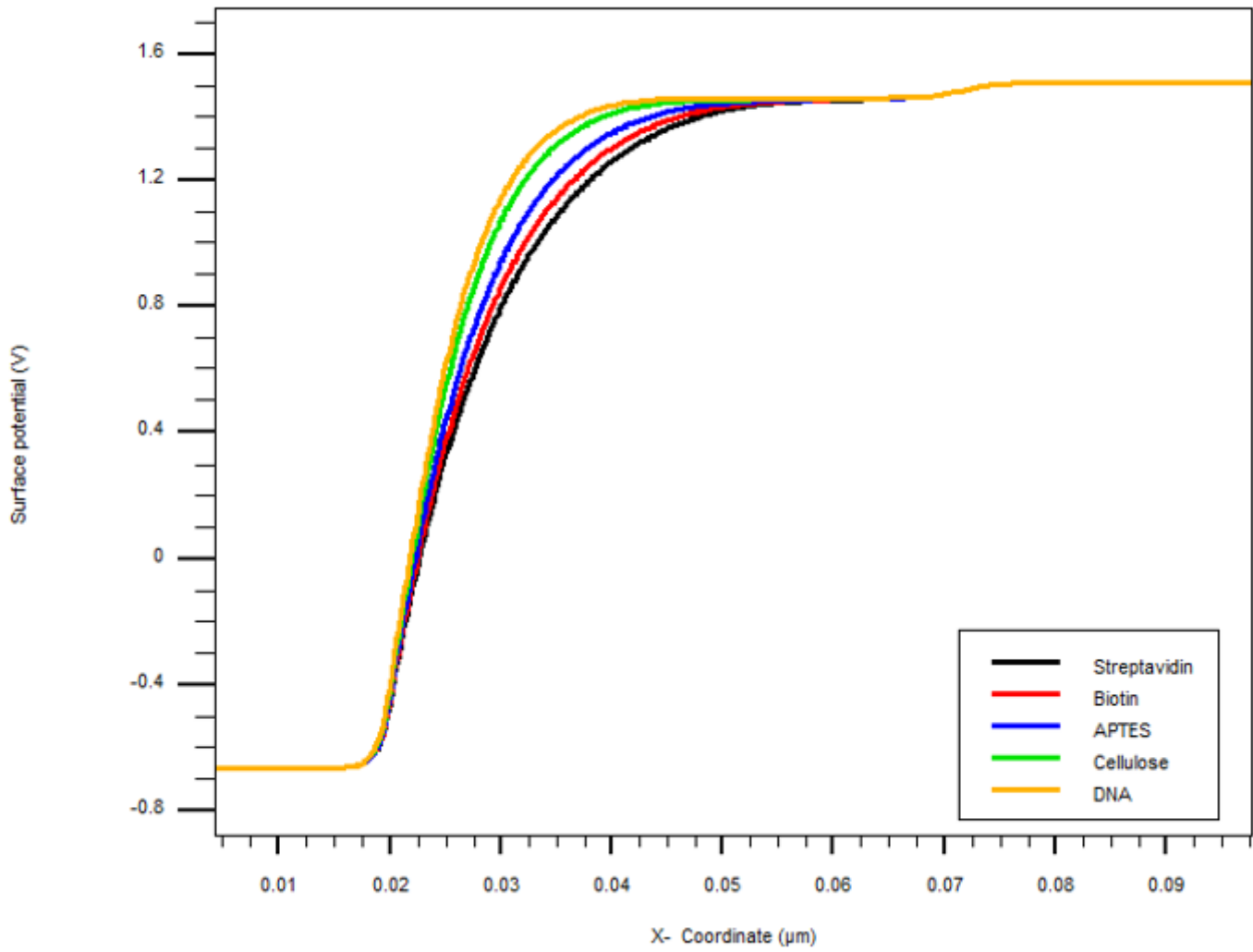


Figure 3

Plot of Surface potential of TFET Biosensor for various biomolecules

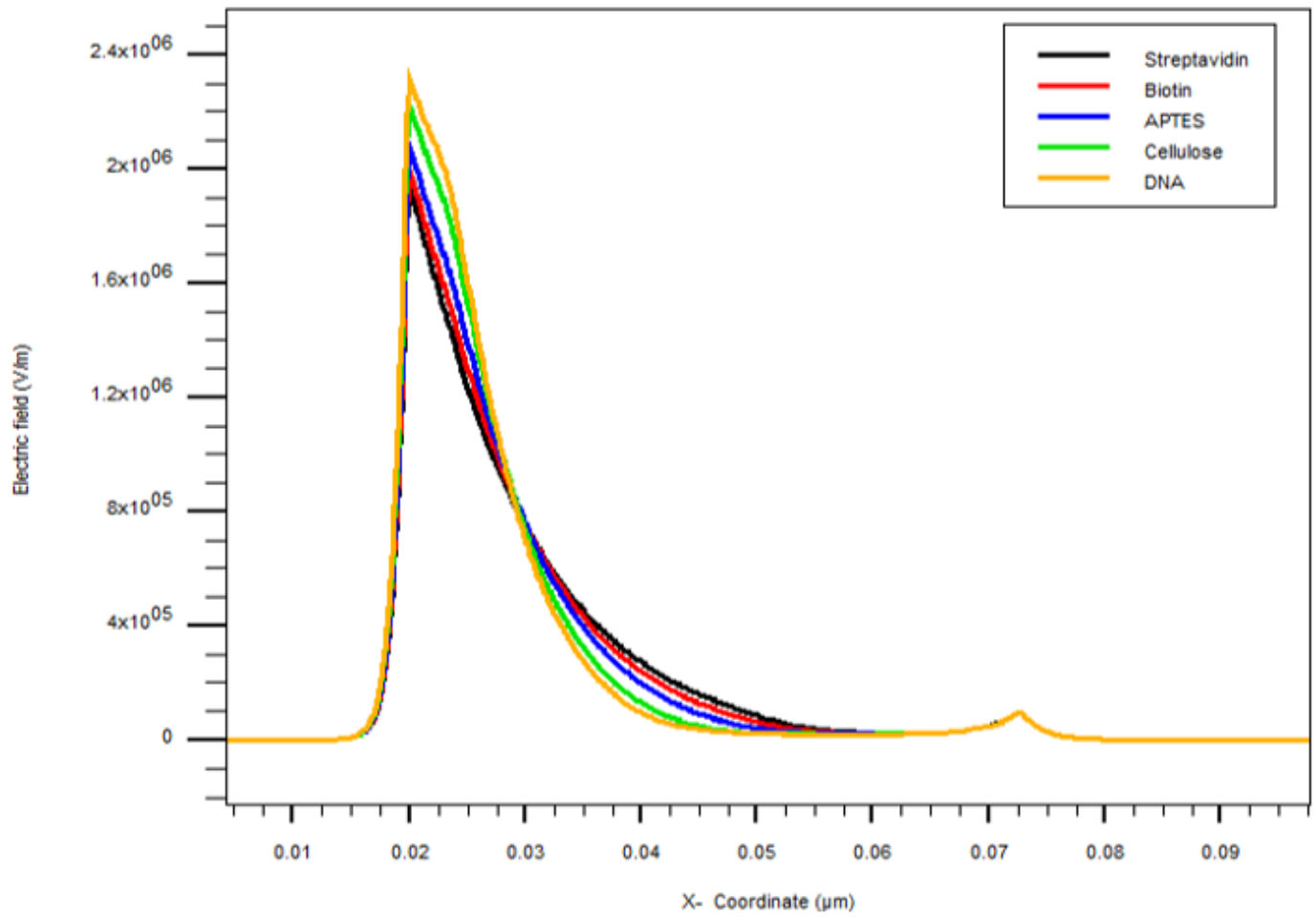


Figure 4

Plot of Electric field of TFET Biosensor for different biomolecules

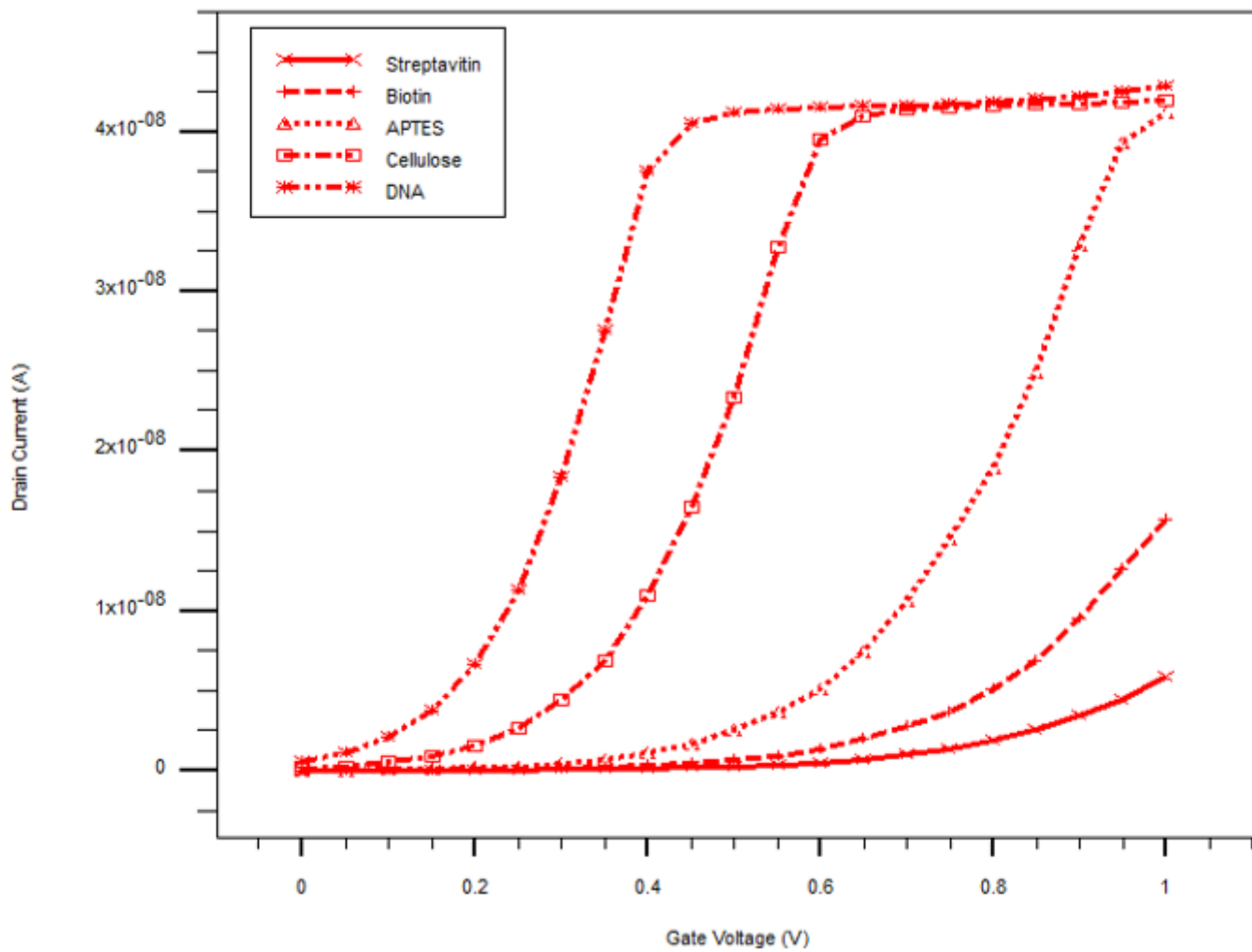


Figure 5

ID v/s VG plot for different Biomolecules

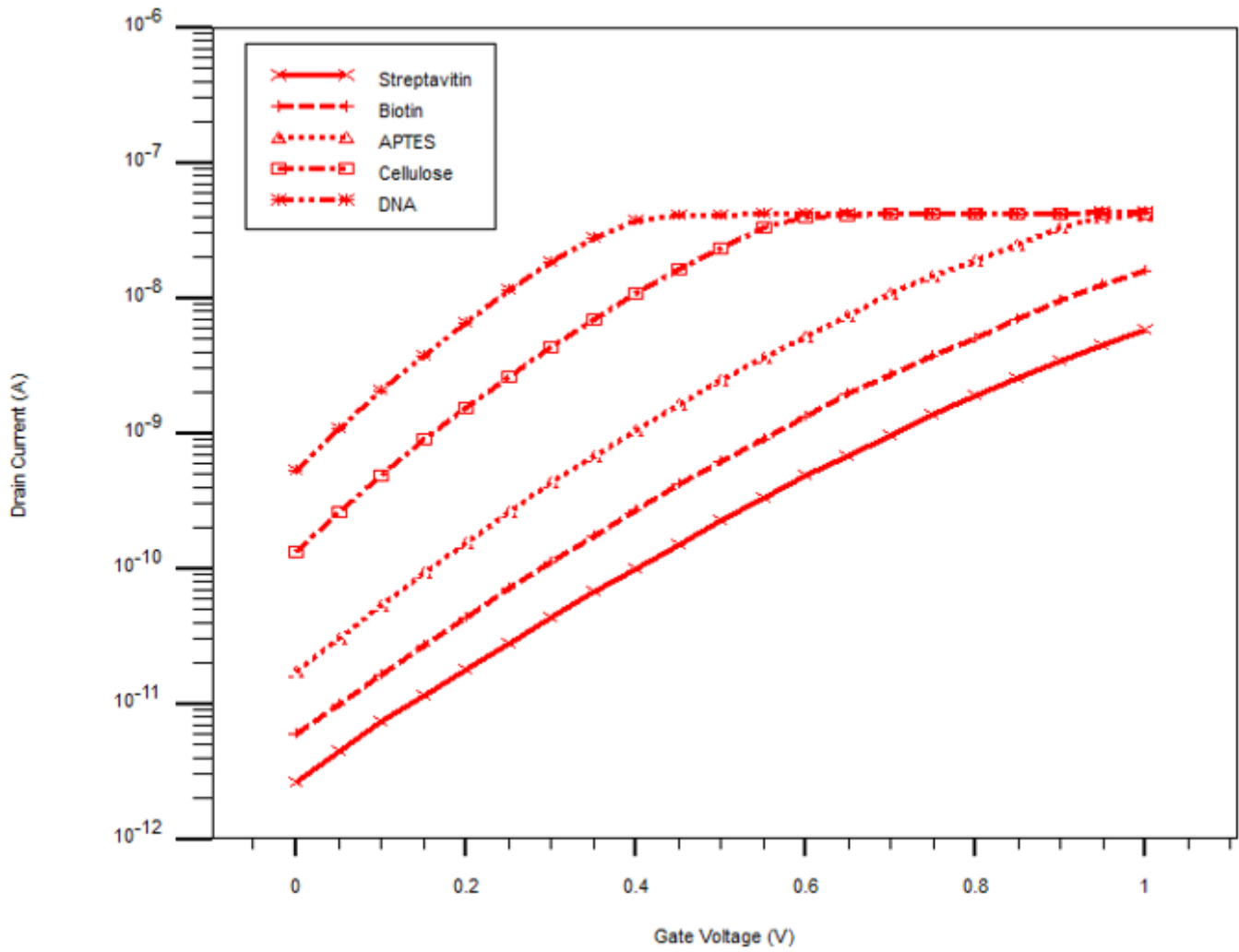


Figure 6

ID v/s VG for change in Biomolecules with different dielectric values (in log scale)

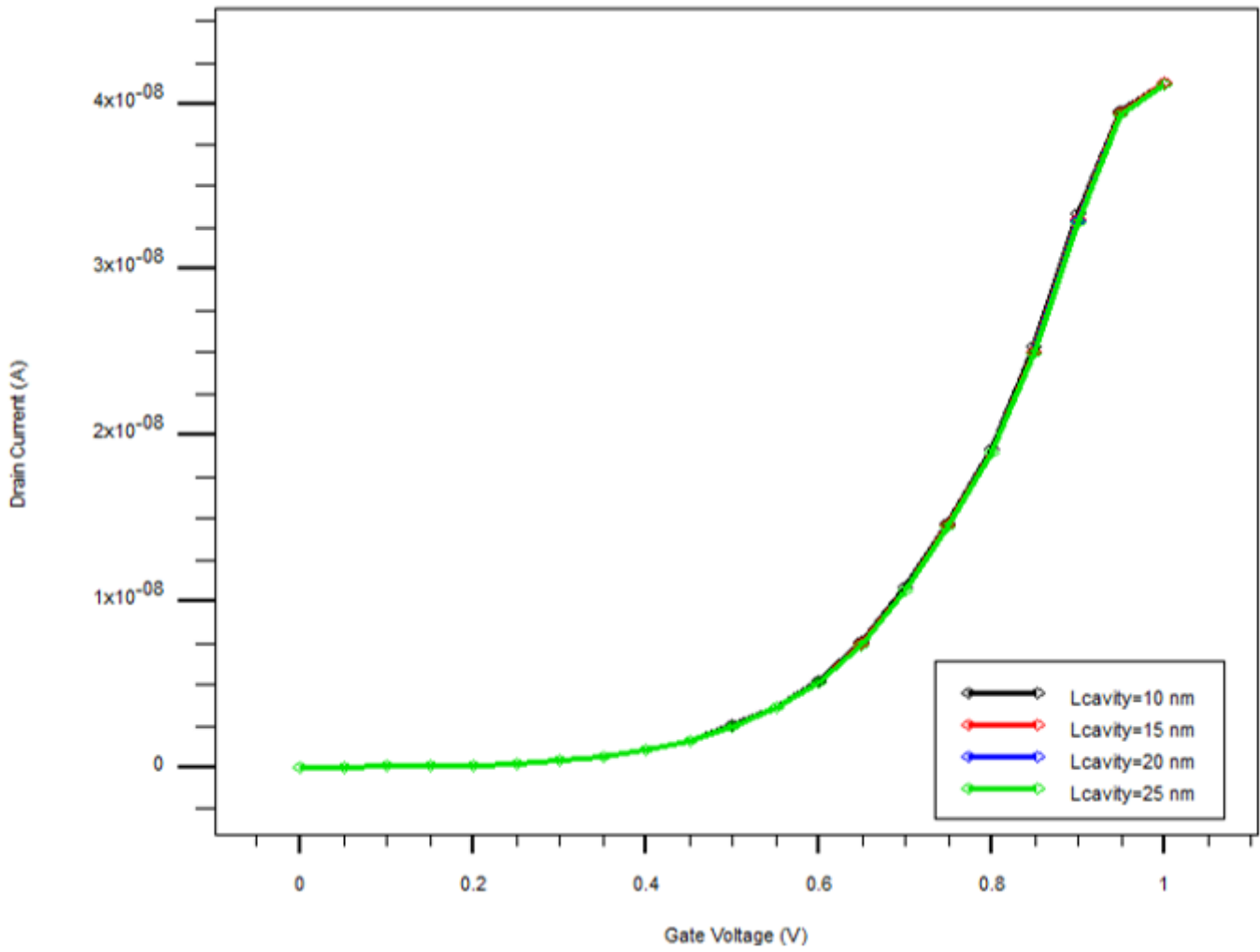


Figure 7

ID v/s VG for change in Length of cavity

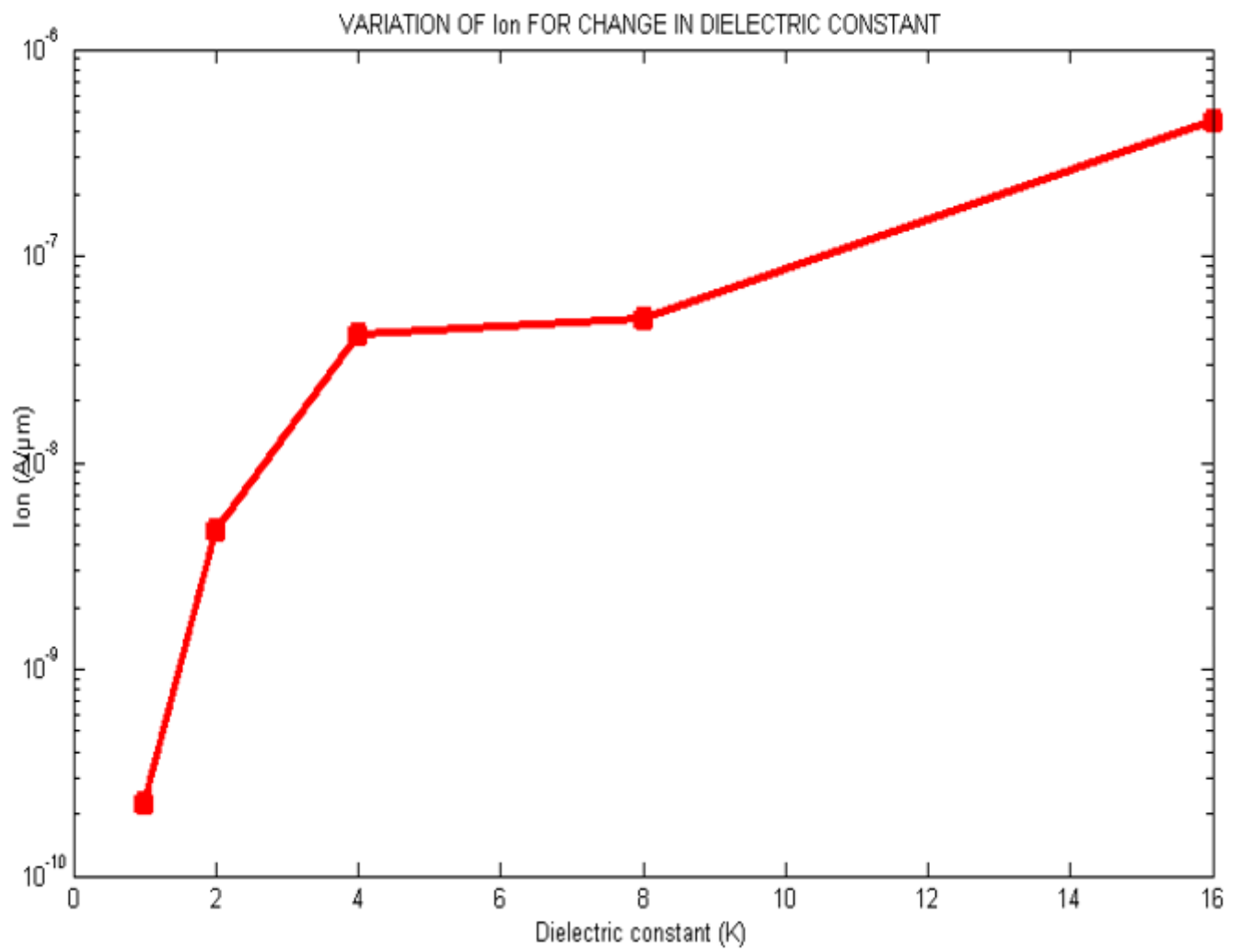


Figure 8

ON current plot for change in Biomolecules with different dielectric values